SUPERFICIAL TUMOR HYPERTHERMIA WITH FLAT LEFT-HANDED METAMATERIAL LENS

Y. Gong and G. Wang

Department of Telecommunication Engineering
Jiangsu University
301 Xuefu Road, Zhenjiang 212013, China

Abstract—Flat left-handed metamaterial (LHM) lens can generate appropriate focusing spot in biological tissue as required in microwave tumor hyperthermia treatment. By using single flat LHM lens to concentrate microwave in a mass of tissue covered by water bolus, microwave hyperthermia scheme is proposed for superficial tumor hyperthermia. The power distribution in tissue is simulated by finite-difference time-domain method, and the thermal pattern is calculated by solving the bio-heat transfer equation. It is demonstrated that, by using a flat LHM lens of thickness of 4 cm to concentrate microwave of 2.45 GHz, a temperature above 42°C can be achieved and maintained in one hour in a tissue region of about 1.0 cm in width and 1.2 cm in depth in tissue with the source amplitude of 43.44 V/cm, which is suitable for superficial tumor hyperthermia. By adjusting the position of microwave source, the heating zone in tissue can be adjusted in both the lateral and depth direction in tissue. The influence of fat layer, effects of water bolus and microwave frequency on hyperthermia, is investigated as well.

1. INTRODUCTION

Microwave hyperthermia has been accepted as an effective adjuvant for malignant tumor treatment. In hyperthermia treatment, temperature in tumor region is generally raised to above 42°C and kept for a sufficient period of time for enough tumor damage, while temperatures below 42°C is desired in tissue surrounding the tumor to avoid normal tissue damage.

For superficial tumor hyperthermia, microwave applicators should have the ability to effectively concentrate microwave energy in a

---

Corresponding author: G. Wang (gwang@ujs.edu.cn).

specific superficial region under skin [1]. Cancerous superficial tumors, such as the recurrent cancers of the breast, chest wall, and skin, generally extend no more than several centimeters beneath the tissue surface [1]. For subcutaneous cancer which occurs in a small region, external single-element applicators such as waveguide [2] and specially designed antennas [3, 4] can be used for hyperthermia treatment. Generally, single-element applicator will provide Gaussian-shaped power distribution with the highest intensity of the beam located directly in front of the applicators. For subcutaneous diffuse recurrence cancer, a relatively large and uniform heating pattern is required. Array applicators such as the printed circuit board array [5] and waveguide slot array [6] can be applied to generate uniform temperature pattern over a relatively large area. Nowadays, microwave hyperthermia has been used for the treatment of superficial malignant tumors in chestwall, neck and axilla region [7–9].

Left-handed metamaterials (LHM) provide new prospects for hyperthermia. It has been demonstrated experimentally that a flat LHM slab can be used as a lens to focus microwave energy emitted from the phase center of microwave antenna and acquire a subwavelength focusing resolution [10, 11]. Although the loss of practical LHM will increase the size of focusing spot of a flat LHM lens and destroy Pendry's perfect lens [12], flat LHM lens shows great potential for microwave hyperthermia due to the convenient adjustment of position of focusing or heating spot in tissue region. For example, by moving the source emitting microwave towards the LHM slab, the focal point on the other side of LHM slab will move apart from the slab. As a result, the heating spot in tissue can be adjusted readily by moving the source, without any complex deployment and control system as required in the conventional array applicator. In addition, microwave focusing spot of moderate size suitable for tumor hyperthermia can be achieved even in heterogeneous lossy medium [13].

Recently, the possibility of hyperthermia by using LHM lens was investigated. Zhao and Cui's simulation results [14] indicated that the specific absorption rate (SAR) of 900 MHz microwave inside a lossy dielectric object can be enhanced tremendously when a flat LHM slab is applied. In [15], Karathanasis et al. reported significantly enhanced SAR in the head model by using a LHM slab in conjunction with a layer of lossless dielectric material. In [16], four-lens LHM applicator was suggested for breast tumor hyperthermia. Different schemes with flat LHM lenses have also been investigated for effective breast tumor microwave hyperthermia [17].

In this paper, the feasibility of single flat LHM lens for hyperthermia of a superficial tumor will be studied by using two-

dimensional (2-D) finite-difference time-domain (FDTD) method. In Section 2, the scheme and numerical model for superficial hyperthermia with flat LHM lens are introduced. In Section 3, the performance of the proposed method is studied, and the method to adjust the heating depth is demonstrated. In Section 4, influence of fat layer, effects of water bolus and microwave frequency on hyperthermia, is further discussed.

2. METHOD

The hyperthermia scheme with a flat LHM lens is shown in Fig. 1. Microwave emitted from a source in front of the LHM slab lens is first concentrated in the LHM lens, and then at point F in tissue. As a demonstration of the feasibility of microwave superficial tumor hyperthermia with LHM lens, we use effective negative permeability and permittivity to define the LHM slab in the model. In our 2-D FDTD simulation, the source is supposed to be a line source set on z-axis in front of the LHM slab lens and extended infinitely in y-direction. Biological tissue to be heated is assumed to be homogeneous, muscle-like tissue covered by a skin layer of 0.2 cm thickness. Under the skin, there may be a fat layer of certain thickness in the tissue. Outside on the skin layer, water bolus of thickness of d_w cm is used to protect the skin from being overheated. The thickness of flat LHM lens is d cm. For practical situation, the tissue could be heterogeneous to some extent. It is reported that tissue heterogeneity of no more than $\pm 50\%$ will not cause significant impacts on the focusing of flat LHM lens except that the focusing point is shifted [13]. Therefore, hyperthermia with a layered homogeneous tissue could be representative.

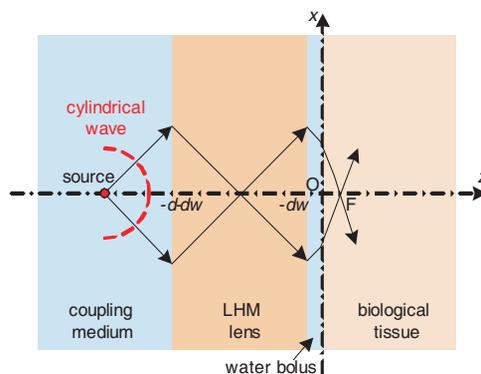For demonstration, we use a frequency of 2.45 GHz for superficial

Figure 1. Hyperthermia scheme by using flat LHM lens.

Table 1. Dielectric properties of simulation model [18].

Material	Relative Permittivity	Conductivity (S/m)
Skin (wet)	42.85	1.59
Fat	4.39	0.08
Muscle*	53	1.81
Water Bolus	80	0.06

*The muscle parameters are the averages of parameters of muscle with parallel and transverse fiber.

hyperthermia. At 2.45 GHz, typical relative permittivity and conductivity of skin, muscle and water bolus at the operating frequency are listed in Table 1.

In the FDTD codes, the artificial LHM is supposed to be isotropic and characterized by relative permittivity ε_{rLHM} and μ_{rLHM} of the form

$$\varepsilon_{rLHM}(\omega) = 1 - \frac{\omega_{pe}^2}{\omega^2 + 2j\delta\omega} \tag{1}$$

$$\mu_{rLHM}(\omega) = 1 - \frac{\omega_{pm}^2}{\omega^2 + 2j\delta\omega} \tag{2}$$

Proper permittivity ε_{rLHM} and permeability μ_{rLHM} of LHM can be defined by setting ω_{pe}, ω_{pm} and loss factor δ in (1) and (2). To match the water bolus, we may set $\omega_{pe}=9\omega$, $\omega_{pm} = 1.414\omega$, $\omega = 2\pi f$ and $\delta = 3.3\times10^5$ (1) and (2) so that $\varepsilon_{rLHM} \approx -80 + j1.4 \times 10^{-3}$, $\mu_{rLHM} \approx -1 + j8.57 \times 10^{-5}$ for the LHM lens. The coupling medium is set to be liquid with $\varepsilon_{rm} = 80$ for impedance matching, and can be circulated so that the source and LHM lens can be cooled.

In the FDTD codes, ten-cell extended uniaxial anisotropic perfectly matched layer and transition layer between the LHM and its surrounding medium is introduced to avoid sharp interface as in [19]. In the FDTD simulation, the computational space is set to be 2000×2000 cells of $\Delta x = \Delta z = 0.01$ cm. The source excitation is set to be turned on slowly by using an exponential ramp function of $(1 - e^{-t/\tau})\sin(\omega t)$ with $\tau = 25 \cdot 2\pi/\omega$ to avoid exciting other frequency components. The time step is 0.236 ps, and 150000 time steps are set to ensure the steady state. For practical application, appropriate lens size can be designed according to the focusing properties of LHM lenses of different sizes as discussed in [20].

3. RESULTS

For demonstration, we use flat LHM lens of thickness $d = 4\,\text{cm}$ and water bolus of thickness of $d_w = 0.5\,\text{cm}$. A line source with input amplitude of $43.44\,\text{V/cm}$ is set at $2\,\text{cm}$ in front of the flat LHM lens, i.e., at $(z = -6.5\,\text{cm}, x = 0)$. Fig. 2 shows the electric field strength and power distribution inside the tissue when a steady state is reached. In Fig. 2, the dashed line depicts the interface between the skin layer and muscle. The peak power distribution is observed at $(z = 0.39\,\text{cm}, x = 0)$, the black-solid line defines the $-3\,\text{dB}$ and $-10\,\text{dB}$ contour line of power distribution in the tissue. By measuring the size of muscle region characterized by the $-3\,\text{dB}$ contour line, an effective heating region of approximately $1.2\,\text{cm}$ in z-direction and $0.8\,\text{cm}$ in x-direction in the tissue is obtained.

The hyperthermia performance characterized by temperature distribution in the tissue can be evaluated by solving Pennes' bio-heat equation (BHE) [21, 22]:

$$C_p(\vec{r})\rho(\vec{r})\frac{\partial T(\vec{r})}{\partial t} = \nabla \cdot \left(K(\vec{r})\nabla T(\vec{r})\right) + A_0(\vec{r}) + Q(\vec{r}) - B(\vec{r})\left(T(\vec{r}) - T_B\right). \tag{3}$$

In the BHE Equation (3), Q is the electromagnetic power distribution, A_0 is the metabolic heat production, B is the heat exchange mechanism due to capillary blood perfusion, C_p is the specific heat capacity, ρ is the tissue density, K is the thermal conductivity,
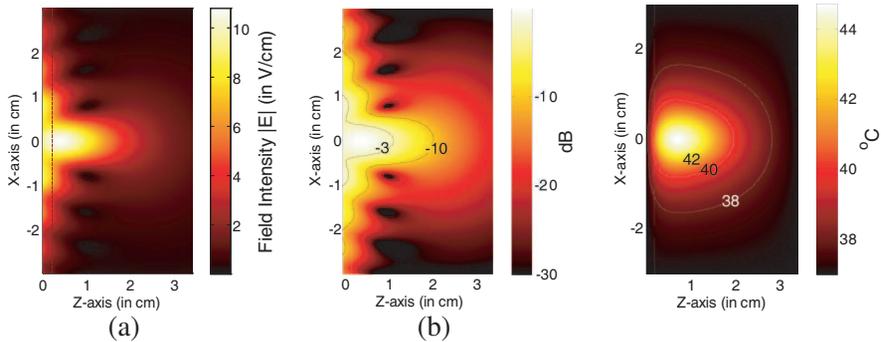

Figure 2. Electric field strength distribution (a) and microwave power deposition (b) in tissue when the source is set at $(z = -6.5\,\text{cm}, x = 0)$.

Figure 3. Temperature distribution in tissue when the source is set at $(z = -6.5\,\text{cm}, x = 0)$.

T_B is the blood temperature assumed to be a constant $37°$C as body temperature. The initial temperature of water bolus and tissue (including muscle temperature) is assumed to be $37°$C. For skin and muscle, the thermal parameters used in (3) are defined as in Table 2.

Figure 3 shows the temperature distribution after one hour heating. The temperature distribution is obtained by solving (3) with finite-differential approach [22]. In Fig. 3, the dashed line defines the interface between skin layer and muscle. From the contour lines in Fig. 3, it is observed that temperature distribution is smoother than that of the power distribution shown in Fig. 2. This can be attributed to the heat diffusion. The highest temperature in the tissue is approximately $44.7°$C at 0.71 cm below the skin surface. Temperature above $42°$C can be achieved and maintained for one hour in a tissue region of about 1.0 cm in width and 1.2 cm in depth. Due to the use of water bolus, the highest temperature of the skin is about $41.2°$C although there is obvious strong power distribution near the skin layer.

Table 2. Thermal parameters of tissue for the BHE [22].

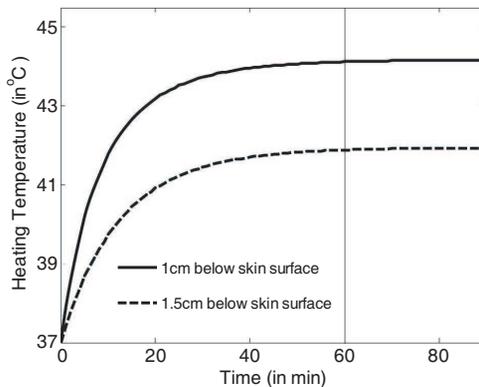|	K (W/m°C)	C_p (J/(kg°C))	A_0 (W/m^3)	B (W/(m^3°C))	ρ (kg/m^3)
Skin	0.42	3500	1620	9100	1100
Fat	0.25	2500	300	1700	1000
Muscle	0.5	3600	480	2700	1050

Figure 4. Temperature rise with the heating time for hyperthermia with LHM lens applicator.

The variation of temperature with heating time at two typical depths in the tissue is shown in Fig. 4. It is observed that there is a fast temperature rise within a heating time of 20 minutes, and the temperature approaches to a steady temperature after 60 minutes heating.

One of the distinct merits of using flat LHM lens is that the focal point can be adjusted in the depth direction by moving the source forwards and backwards. In the superficial hyperthermia treatment, the depth of effective heating spot can be adjusted by changing the source position. For the system with a 4 cm-thick LHM lens and 0.5 cm-thick water bolus, the focal point can be adjusted in a range no more than 3.5 cm depth in the tissue. Figs. 2 and 3 depict the power distribution and temperature distribution when the source is set at $(z = -6.5\,\text{cm}, x = 0)$. For comparison, hyperthermia with two other typical source positions is considered.

Figure 5 shows the power distribution and corresponding temperature distribution in tissue when the source is set at $(z = -7.5\,\text{cm}, x = 0)$. The dashed lines indicate the interface between the skin and muscle. The expected focal point is around skin surface, which indicates a relative shallow hyperthermia, as shown in Fig. 5(a). In Fig. 5(b), the highest temperature is measured at 0.50 cm below the skin surface.

Figure 6 shows the power distribution and corresponding temperature distribution in tissue when the source is set at $(z = -5.5\,\text{cm}, x = 0)$. The dashed lines indicate the interface between the skin and muscle. The expected focal point is around $(z = 0.98\,\text{cm}, x = 0)$, which indicates a relative deep hyperthermia, as shown in Fig. 6(a). It is observed in Fig. 6(b) that the highest temperature is measured at $(z = 1.10\,\text{cm}, x = 0)$.
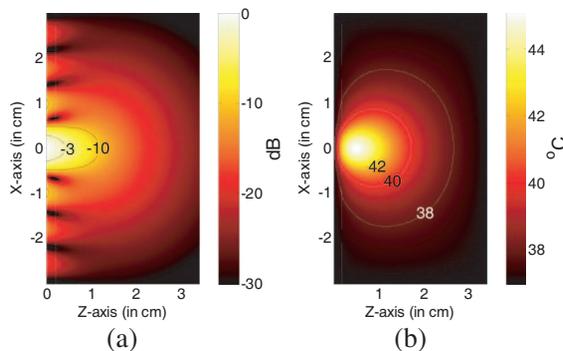

Figure 5. Power distribution (a) and temperature distribution (b) in tissue when the source is set at $(z = -7.5\,\text{cm}, x = 0)$.
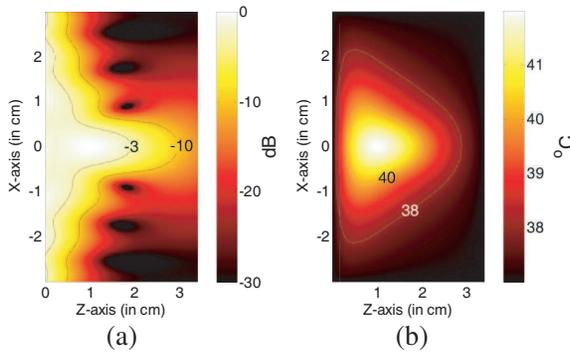
Figure 6. Power distribution (a) and temperature distribution (b) in tissue when the source is set at ($z = -5.5$ cm, $x = 0$).

Table 3.   Performance of hyperthermia for source at different positions.

source positions on z-axis	$z = -7.5$ cm	$z = -6.5$ cm	$z = -5.5$ cm
42°C region in z-direction (in cm)	1.07	1.21	—
42°C region in x-direction (in cm)	0.97	0.99	—
highest temperature in skin	42.89°C	41.15°C	39.04°C
temperature at 1 cm in tissue	43.22°C	44.12°C	41.98°C
highest temperature on z axis	45.09°C at $z = 0.50$ cm	44.70°C at $z = 0.71$ cm	41.98°C at $z = 1.01$ cm

Comparison of power distribution and temperature distribution shown in Figs. 2, 3, 5, and 6 indicates that as the source moving towards the entrance surface of the LHM lens, the heating depth increases, and the -3 dB contour region in power distribution also increases. The effective treatment area in width and depth and corresponding temperature in skin and muscle are listed in Table 3.

We note that when the source is set at ($z = -5.5$ cm, $x = 0$), the heating pattern in Fig. 6(b) has a relatively lower temperature distribution. The reason is that this scenario represents relatively deep heating so that microwave energy suffers much dissipation before focusing. For deep heating, we may raise the input power in order to obtain necessary therapeutic temperature.

4. DISCUSSION

4.1. Influence of Fat Layer

For most biological tissue on the trunk, there is a fat layer under skin. The fat layer may have different thicknesses, depending on the position of region to be heated. Typical dielectric parameters at 2.45 GHz for fat layer have been listed in Table 1. Large dielectric contrast between the fat layer and the skin or muscle can be observed. As a result, strong reflection will occur when microwave propagates across the skin-fat and fat-muscle interfaces. The amount of power deposited in the skin and muscle will be different from those given in Section 3. As a result, the hyperthermia performance of flat LHM lens will be modified.
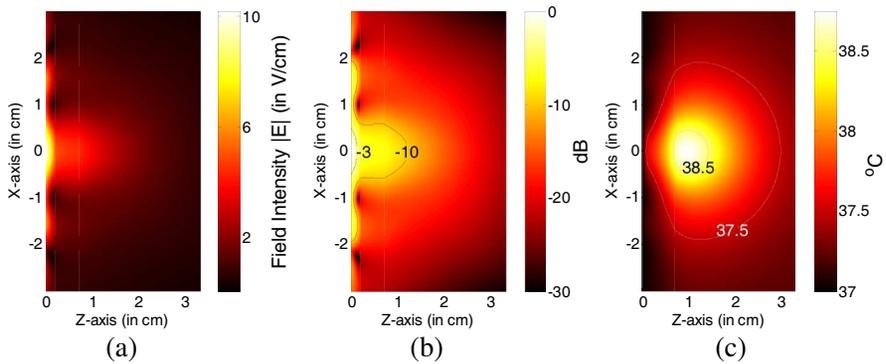

Figure 7. Field strength distribution (a), localized power distribution (b) and localized temperature distribution (c) in tissue when there is a 0.5 cm-thick fat layer.
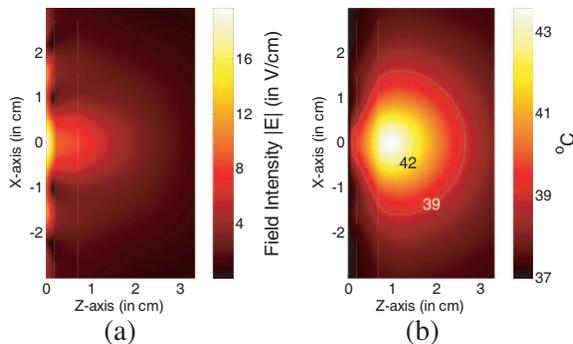

Figure 8. Electric field strength distribution (a) and temperature distribution (b) in tissue when source amplitude of 83.94 V/cm is applied.

For illustration, we include a fat layer of thickness of 5 mm between the skin and the muscle in the model we simulated in Section 3. When a line source with input amplitude of 43.44 V/cm is set at 2 cm in front of the flat LHM lens, i.e., at ($z = -6.5$ cm, $x = 0$) in the model shown in Fig. 2, the field distribution, power distribution and the temperature distribution in the tissue are shown in Figs. 7(a), (b) and (c), respectively. In these figures, the fat layer is defined between the two dashed lines. The left dashed line indicates the interface between skin and fat layer, the right dashed line indicates the interface between fat layer and muscle.

It is observed in Fig. 7(b) that the -3 dB region of power deposition is kept in the skin layer due to strong reflection at the skin-fat interface. In Fig. 7(c), the highest temperature recorded in tissue is approximately 38.75°C. In the skin layer, the highest temperature is about 37.71°C.

To realize the desired hyperthermia treatment, we must increase the input power of source. For line source of 83.94 V/cm, the temperature distribution in the tissue after 60 minutes heating is shown in Fig. 8. It is observed that the highest temperature can be recorded at 0.24 cm under the fat-muscle interface in the muscle, which reads to be approximately 43.57°C. Temperature above 42°C can be achieved and maintained for one hour in a tissue region of about 1.16 cm in width and 0.87 cm in depth, while in the skin layer the highest temperature is about 39.68°C.

Therefore, by increasing the input power of microwave source, superficial hyperthermia can be performed in case there is a fat layer.

4.2. Effects of Water Bolus

Employing water bolus may have several advantages when performing superficial tumor hyperthermia. First, water bolus serves as a good heat exchanger to keep skin from being overheated. Second, water bolus may serve as a coupling medium between the antenna and skin [23]. It is pointed out in [24] that there is a frequency-dependant critical thickness for water bolus coupling layers for the antenna array to avoid causing perturbation to the SAR pattern. For hyperthermia with flat LHM lens, the effects of water bolus on hyperthermia performance should be investigated as well.

To be representative, the 4 cm-thick LHM slab is set on water bolus layer of two other thickness of $d_w = 0.1$ cm and $d_w = 0.9$ cm, respectively. The source is fixed at 2 cm in front of the LHM lens. For comparison, a line source of amplitude of 43.44 V/cm as above is applied.
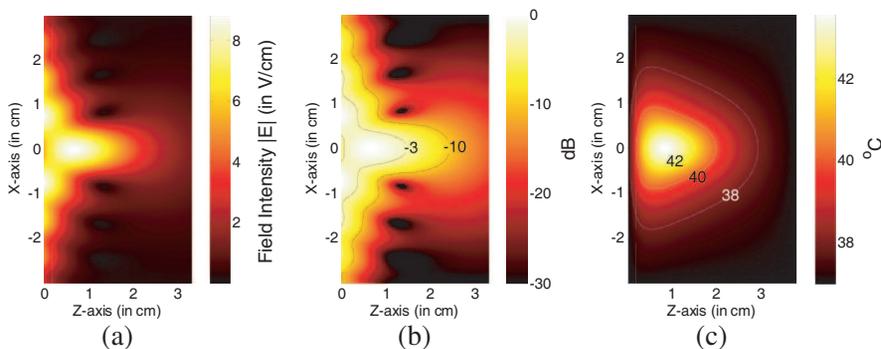
Figure 9. Electric field strength distribution (a), localized power distribution (b), and localized temperature distribution (c) in tissue when there is a 0.1 cm-thick water bolus.

Figure 10. Electric field strength distribution (a), localized power distribution (b), and localized temperature distribution (c) in tissue when there is a 0.9 cm-thick water bolus.
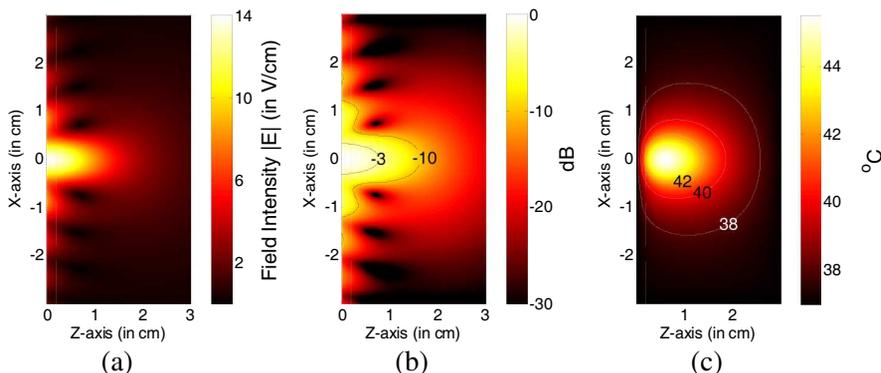
Figure 9 shows the calculated power deposition and temperature distribution in tissue when the 0.1 cm-thick water bolus is applied, where the dash line indicates the skin surface. Compared with that shown in Fig. 2 and Fig. 3, more power deposition and deeper penetration can be observed. The highest temperature in Fig. 9(c) is recorded to be approximately $43.57°C$ at 0.62 cm under the skin-muscle interface in muscle.

Figure 10 shows the calculated power deposition and temperature distribution inside tissue when the 0.9 cm-thick water bolus is applied. Compared with the temperature distribution in Fig. 9(c), the effective treatment region now becomes a circular one as the thickness of water

bolus increase, which accords with what has been observed in [25]. In this case, the highest temperature is recorded at $0.40\,$cm under the skin-muscle interface in muscle, and raised to $45.51°$C.

Therefore, the water bolus will introduce change to both the power deposition pattern and the temperature distribution. The position where the highest temperature is recorded approaches to the skin-muscle interface. To show more details, several other values of the bolus thickness are considered, and the results are listed in Table 4. We have the observation that there is an optimal thickness of water bolus for the LHM lens and source deployment. When water bolus of thickness around $0.9\,$cm is applied, the highest temperature and largest heating area of temperature above $42°$C can be obtained.

To show what happened during the increasing of water bolus thickness, Fig. 11 depicts the field strength distribution in water bolus and tissue when different water bolus thickness is considered. In the simulation, the source-lens distance is set to be $2\,$cm.

From Fig. 11, we have the following observation. When a thin water bolus is applied, microwave fields suffer from reflection occurred at the interface between water bolus and skin before the focusing spot is developed in tissue. As a result, the field strength at the focusing spot is limited to some extent. When a thick water bolus is applied, the focusing spot are formed in water, not in tissue. Therefore, the power deposition in tissue gains less from focusing of LHM lens applicator. When water bolus of proper thickness is applied, some fields are reflected and most of them contribute to the forming of focusing spot in tissue. As a result, higher power deposition and thus better hyperthermia can be generated in tissue.

Table 4.

thickness of water bolus	$d_w = 0.1\,$cm	$d_w = 0.3\,$cm	$d_w = 0.5\,$cm	$d_w = 0.7\,$cm	$d_w = 0.9\,$cm
$42°$C region in z-direction (in cm)	1.04	1.14	1.21	1.23	1.20
$42°$C region in x-direction (in cm)	0.87	0.94	0.99	1.00	1.01
highest temperature in skin	$39.96°$C	$40.53°$C	$41.15°$C	$41.80°$C	$42.42°$C
temperature at 1 cm in tissue	$43.53°$C	$43.87°$C	$44.12°$C	$44.23°$C	$44.20°$C
highest temperature on z axis	$43.57°$C at $z = 0.82\,$cm	$44.13°$C at $z = 0.76\,$cm	$44.70°$C at $z = 0.71\,$cm	$45.15°$C at $z = 0.65\,$cm	$45.51°$C at $z = 0.60\,$cm

| thickness of water bolus	$d_w = 1.1\,$cm	$d_w = 1.3\,$cm	$d_w = 1.5\,$cm	$d_w = 1.7\,$cm	$d_w = 1.9\,$cm
$42°$C region in z-direction (in cm)	1.18	1.12	1.03	0.89	0.72
$42°$C region in x-direction (in cm)	1.01	0.98	0.95	0.87	0.74
highest temperature in skin	$42.86°$C	$43.04°$C	$42.96°$C	$42.48°$C	$41.92°$C
temperature at 1 cm in tissue	$43.96°$C	$43.55°$C	$43.04°$C	$43.40°$C	$41.69°$C
highest temperature on z axis	$45.63°$C at $z = 0.55\,$cm	$45.48°$C at $z = 0.51\,$cm	$45.08°$C at $z = 0.49\,$cm	$44.33°$C at $z = 0.48\,$cm	$43.49°$C at $z = 0.47\,$cm
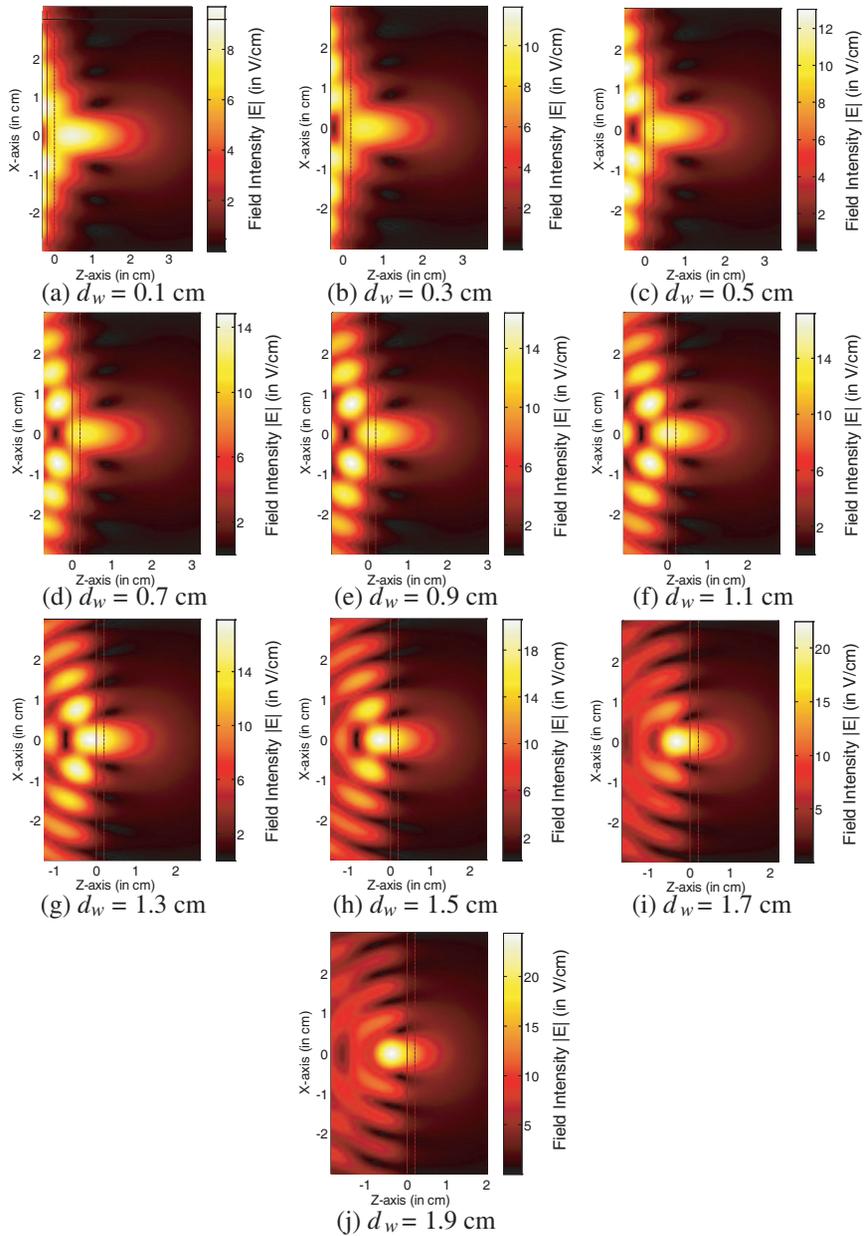
Figure 11. Electric field strength distribution in water bolus and tissue when water bolus of different thickness is applied.

4.3. Hyperthermia with Lower Frequency

As is well-known, microwave of lower frequency suffers less tissue attenuation. Therefore, by using microwave of 915 MHz or 433 MHz, deeper and larger heating zone in tissue can be expected.

For comparison, Figs. 12(a) and (b) show the temperature distribution of hyperthermia with microwave of 2.45 GHz and 915 MHz, respectively. In the simulations, the source is set at 2 cm in front of the 4 cm thick LHM slab, and a 5 mm water bolus, 2 mm skin layer and 5 mm fat layer are considered. For 915 MHz hyperthermia, corresponding water and tissue dielectric parameters at 915 MHz are applied.

In Fig. 12(a), the amplitude of the 2.45 GHz microwave source is set to be 83.94 V/cm. The highest temperature is 43.57°C at 0.24 cm under the fat-muscle interface. The above 42°C region is 0.87 cm in z-direction and 1.16 cm in x-direction.

In Fig. 12(b), the amplitude of the 915 MHz microwave source is set to be 36.32 V/cm. The highest temperature is 43.42°C at 0.55 cm under the fat-muscle interface. The above 42°C region is 1.65 cm in z-direction and 2 cm in x-direction.

Therefore, by using 915 MHz microwave, although small source excitation is applied, larger and deeper heating zone can be observed.
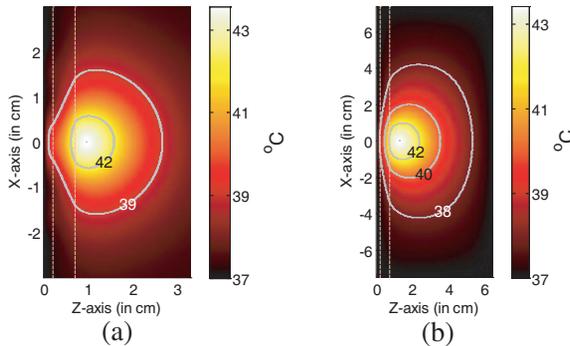

Figure 12. Temperature distribution of hyperthermia with microwave of 2.45 GHz (a) and 915 MHz (b).

5. CONCLUSION

Superficial hyperthermia utilizing left-handed material (LHM) slab lens is demonstrated. The temperature distribution in tissue obtained by FDTD simulation indicates that flat LHM lens can be used

as a candidate for superficial hyperthermia applicator. Due to the concentration of microwave power in tissue, different power deposition and temperature distribution pattern can be obtained if compared to that generated by antenna applicator. By moving the source, the heating zone in tissue can be easily adjusted. Since the feasibility of microwave hyperthermia depends on the generation of a heating /focusing spot at tumor position in biological tissue, isotropic flat LHM lens with experimentally-confirmed LHM permittivity and permeability at the operation frequency will work as well. For such LHM lens, the coupling medium (liquid, maybe including the bolus between the lens and skin) should be properly selected to reduce the reflection loss. It should be further remarked that LHM hyperthermia with lower operation frequencies (such as 433 MHz and 915 MHz) can also be considered when deeper heating depth under skin is desired, if specific LHM lens can be fabricated at these frequencies.

ACKNOWLEDGMENT

REFERENCES

1. Vernon, C. C., J. W. Hand, S. B. Field, D. Machin, J. B. Whaley, J. Van Der Zee, W. L. J. Van Putten, G. C. Van Rhoon, J. D. P. Van Dijk, D. G. González, F. Liu, P. Goodman, and M. Sherar, "Radiotherapy with or without hyperthermia in the treatment of superficial localized breast cancer: Results from five randomized controlled trials," *Int. J. Radiat. Oncol. Biol. Phys.*, Vol. 35, No. 4, 731–744, 1996.

2. Rietveld, P. J. M., W. L. J. Van Putten, J. Van Der Zee, and G. C. Van Rhoon, "Comparison of the clinical effectiveness of the 433 MHz Lucite cone applicator with that of a conventional waveguide applicator in applications of superficial hyperthermia," *Int. J. Radiat. Oncol. Biol. Phys.*, Vol. 43, No. 3, 681–687, 1999.

3. Montecchia, F., "Microstrip-antenna design for hyperthermia treatment of superficial tumors," *IEEE Trans. Biomed. Eng.*, Vol. 39, No. 6, 580–588, 1992.

4. Prior, M. V., M. L. D. Lumori, J. W. Hand, G. Lamaitre, C. J. Schneider, and J. D. P. van Dijk, "The use of a current sheet applicator array for superficial hyperthermia: Incoherent versus

coherent operation," *IEEE Trans. Biomed. Eng.*, Vol. 42, No. 7, 694–698, 1995.

5. Jacobsen, S., P. R. Stauffer, and D. G. Neuman, "Dual-mode antenna design for microwave heating and noninvasive thermometry of superficial tissue disease," *IEEE Trans. Biomed. Eng.*, Vol. 47, No. 11, 1500–1509, 2000.

6. Gupta, R. C. and S. P. Singh, "Elliptically bent slotted waveguide conformal focused array for hyperthermia treatment of tumors in curved region of human body," *Progress In Electromagnetics Research*, PIER 62, 107–125, 2006.

7. Jones, E. L., J. R. Oleson, L. R. Prosnitz, T. V. Samulski, Z. Vujaskovic, D. Yu, L. L. Sanders, and M. W. Dewhirst, "Randomized trial of hyperthermia and radiation for superficial tumors," *J. Clinical Oncol.*, Vol. 23, No. 13, 3079–3085, 2005.

8. Kapp, D. S., "Efficacy of adjuvant hyperthermia in the treatment of superficial recurrent breast cancer: Confirmation and future directions," *Int. J. Radiat. Oncol. Biol. Phys.*, Vol. 35, No. 5, 1117–1121, 1996.

9. Lee, H. K., A. G. Antell, C. A. Perez, W. L. Straube, G. Ramachandran, R. J. Myerson, B. Emami, E. P. Molmenti, A. Buckner, and M. A. Lockett, "Superficial hyperthermia and irradiation for recurrent breast carcinoma of the chest wall: Prognostic factors in 196 tumors," *Int. J. Radiat. Oncol. Biol. Phys.*, Vol. 40, No. 2, 365–75, 1998.

10. Aydin, K., I. Bulu, and E. Ozbay, "Subwavelength resolution with a negative-index metamaterial superlens," *Appl. Phys. Lett.*, Vol. 90, No. 25, 254102, 2007.

11. Zhu, J. and G. V. Eleftheriades, "Experimental verification of overcoming the diffraction limit with a volumetric Veselago-Pendry transmission-line lens," *Phy. Rev. Lett.*, Vol. 101, No. 1, 013902, 2008.

12. Pendry, J. B. and S. A. Ramakrishna, "Refining the perfect lens," *Physica B*, Vol. 338, No. 1, 329–332, 2003.

13. Wang, G., J. R. Fang, and H. J. Wang, "Focusing of a flat left-handed metamaterial lens in a heterogeneous and lossy medium," *Chin. Phys. Lett.*, Vol. 26, No. 5, 057801, 2009.

14. Zhao, L. and T. J. Cui, "Enhancement of specific absorption rate in lossy dielectric objects using a slab of left-handed material," *Phys. Rev. E*, Vol. 72, No. 6, 061911, 2005.

15. Karathanasis, K. T., I. S. Karanasiou, and N. K. Uzunoglu, "Enhancing the focusing properties of a prototype non-invasive

brain hyperthermia system: A simulation study," *Proc. Ann. Int. Conf. IEEE Engineering in Medicine and Biology Society*, 218–221, 2007.

16. Wang, G. and Y. Gong, "Metamaterial lens applicator for microwave hyperthermia of breast cancer," *Int. J. Hyperthermia*, Vol. 25, No. 6, 434–455, 2009.

17. Wang, G., Y. Gong, and H. J. Wang, "Schemes of microwave hyperthermia by using flat left-handed material lenses," *Microwave and Opt. Tech. Lett.*, Vol. 51, No. 7, 1738–1743, 2009.

18. FCC, Body tissue dielectric parameters tool. http://www.fcc.go -v/oet/rfsafety/dielectric.html.

19. Zhao, Y., P. Belov, and Y. Hao, "Accurate modeling of the optical properties of left-handed media using a finite-difference time-domain method," *Phys. Rev. E*, Vol. 75, No. 3, 037602, 2007.

20. Wang, G., Y. Gong, and H. J. Wang, "On the size of left-handed material lens for near-field target detection by focus scanning," *Progress In Electromagnetics Research*, PIER 87, 345–361, 2008.

21. Pennes, H. H., "Analysis of tissue and arterial blood temperatures in the resting human forearm," *J. Appl. Physiol*, Vol. 85, No. 1, 5–34, 1998.

22. Bernardi, P., M. Cavagnaro, S. Pisa, and E. Piuzzi, "Specific absorption rate and temperature elevation in a subject exposed in the far-field of radio-frequency sources operating in the 10–900-MHz range," *IEEE Trans. Biomed. Eng.*, Vol. 50, No. 3, 295–304, 1998.

23. Neuman, D. G., P. R. Stauffer, S. Jacobsen, and F. Rossetto, "SAR pattern perturbations from resonance effects in water bolus layers used with superficial microwave hyperthermia applicators," *Int. J. Hyperthermia*, Vol. 18, No. 3, 180–193, 2002.

24. Gelvich, E. A. and V. N. Mazokhin, "Resonance effects in applicators water boluses and their influence on SAR distribution patterns," *Int. J. Hyperthermia*, Vol. 16, No. 2, 113–128, 2000.

25. Ebrahimi-Ganjeh, M. A. and A. R. Attari, "Study of water bolus effect on SAR penetration depth and effective field size for local hyperthermia," *Progress In Electromagnetics Research B*, Vol. 4, 273–283, 2008.